CHECK ONE:

[_X_]Contributor-owned work

Contributor's signature _____ Date _____

Hitoshi Hotokezaka, PhD, DDS

Type or print name and title

Co-contributor's signature _____ Date _____

Type or print name and title

ATTACH ADDITIONAL SIGNATURE PAGE AS NECESSARY

[____]Company/Institution-owned work (made-for-hire in the course of employment)

Company or Institution (Employer-for-Hire) _____ Date _____

Authorized signature of Employer _____ Date _____

[____]**U.S. Government work**

Note to U.S. Government Employees

A Contribution prepared by a U.S. federal government employee as part of the employee's official duties, or which is an official U.S. Government publication is called a "U.S. Government work," and is in the public domain in the United States. In such case, the employee may cross out Paragraph A.1 but must sign and return this Agreement. If the Contribution was not prepared as part of the employee's duties or is not an official U.S. Government publication, it is not a U.S. Government work.

[____]**U.K. Government work (Crown Copyright)**

Note to U.K. Government Employees

The rights in a Contribution prepared by an employee of a U.K. government department, agency or other Crown body as part of his/her official duties, or which is an official government publication, belong to the Crown. In such case, the Publisher will forward the relevant form to the Employee for signature.

Available online at www.sciencedirect.com
SCIENCE DIRECT
Vaccine 24 (2006) 4969–4974
Vaccine
www.elsevier.com/locate/vaccine

Identification of two subpopulations of Bacillus Calmette-Guérin (BCG) Tokyo172 substrain with different RD16 regions

Ikuro Honda [a,*], Masaaki Seki [a], Noriko Ikeda [a], Saburo Yamamoto [b], Ikuya Yano [a], Akira Koyama [a], Ichiro Toida [a]

[a] *Central Laboratory, Japan BCG Laboratory, 3-1-5 Matsuyama, Kiyose City, Tokyo 204-0022, Japan*
[b] *Laboratory of Tuberculosis Control, Department of Bacterial Pathogenesis and Infection Control, National Institute of Infectious Diseases, 4-7-1 Gakuen, Musashimurayama City, Tokyo 208-0011, Japan*

Received 10 May 2005; received in revised form 24 February 2006; accepted 18 March 2006
Available online 4 April 2006

Abstract

Two types of colonies with different morphologies (smooth: S and rough: R) formed when Bacillus Calmette-Guérin (BCG) Tokyo172 substrain was cultured on Middlebrook 7H10 agar medium, and their genotypes were analyzed by multiplex PCR on five RD regions and SenX3-RegX3. In most cases these two colony types had different genotypes, i.e., S colonies showed a characteristic 22 bp deletion in *Rv3405c* of the RD16 region (type I), and R colonies did not have this deletion (type II) similar to many other BCG substrains. Thus, there was a strong relationship between colony morphology and genotype. Both genotypes were found in every Tokyo172 preparation tested, including the seed lot for production, the origin of seed lot from the 1960s and ATCC BCG Japan. Type I was always in the majority. It was suggested that types I and II constituted independent subpopulations within the Tokyo172 substrain. Type I was shown to have a growth advantage over type II both on culture media and in mice organs.

Keywords: BCG Tokyo172; RD16 genotype; Subpopulations

1. Introduction

Shortly after Bacillus Calmette-Guérin (BCG) started to be used as a prophylactic vaccine for tuberculosis, dissociations of BCG into several colony morphologies were reported and their relevance to virulence discussed [1–3]. This was also suggested after BCG was distributed to many countries and various substrains (or daughter strains, such as Pasteur, Danish, Russia or Japan) were established, as Osborn have reported the presence of minor populations showing different colony morphologies, in the Japanese and Danish substrains [4]. We have also found differences of colony morphology when the Tokyo172 substrain is cultured on Middlebrook 7H10 agar medium. As for genetic differences, Bedwell et al. recently reported that there were two genotypes in the commercial Japan (Tokyo172) preparation, which differed in the presence or absence of 22 bp deletion in RD16, in a study to differentiate BCG substrains by using multiplex PCR on RD regions and SenX3-RegX3 [5]. RD16 is one of the several deletions found in BCG compared with *Mycobacterium tuberculosis* H37Rv, of 7608 bp size and containing six ORFs (*Rv3400–Rv3405c*) [6]. RD16 is totally absent from BCG Moreau [6], while present in all other BCG substrains. Bedwell et al. could not find a genotype without 22 bp deletion of RD16 in ATCC BCG Japan, so they implied that the presence of this genotype in commercial preparation might have been caused by the inadvertent contamination of another BCG substrain. This genotype was shown to have a multiplex PCR pattern identical to that of BCG Birkhaug. The presence of two genotypes in a BCG substrain was also suggested by them for the Copenhagen

* Corresponding author. Tel.: +81 424 91 0611; fax: +81 424 92 9752.
E-mail address: honda@bcg.gr.jp (I. Honda).

0264-410X/$ – see front matter © 2006 Elsevier Ltd. All rights reserved.
doi:10.1016/j.vaccine.2006.03.055

(Danish) substrain, with differences in SenX3-RegX3 [5]. Another reported mutation concerning the presence of multiple genotypes in a BCG substrain is tandem duplications, i.e., DU1 is specific to BCG Pasteur and DU2 is considered to exist in all BCG substrains with different sizes, while both double and triple DU2 are suggested to exist in the Pasteur substrain [7,8].

In the present study we investigated the possible relationship between differences of colony morphology and the genotype of the Tokyo172 substrain, as well as whether these different genotypes were originally present in the Tokyo172 substrain or not.

2. Materials and methods

2.1. Bacteria

Lyophilized preparations of BCG vaccine final products made from Tokyo172 substrain (Japan BCG Laboratory Inc., Tokyo, Japan), the seed lot used for production, stock of Tokyo172 from the 1960s which was used to establish the seed lot (origin of seed lot), ATCC BCG Japan (ATCC35737), BCG Birkhaug (ATCC35731), and BCG Pasteur (ATCC35734), were used. *M. tuberculosis* Aoyama B strain was obtained from the Japanese National Institute of Health as a control for PCR analysis.

2.2. Culture of BCG

Middlebrook 7H10 agar medium supplemented with OADC, 7H9 liquid medium (containing 0.05% Tween80) supplemented with ADC (Japan Becton Dickinson Inc., Tokyo, Japan), Sauton's medium (prepared in our laboratory), and Kudoh PD (egg slant) medium (Japan BCG Laboratory Inc., Tokyo, Japan) were used for culture. For serial passaging, the bacteria grown for 2 weeks on each medium were all harvested and mixed, after which a portion was inoculated into the new medium. All cultures were done at 37 °C.

2.3. Multiplex and RD16 PCR analysis

DNA was extracted using a DNA extraction kit (ISOPLANT, Nippon Gene Co. Ltd., Tokyo, Japan) according to the manufacturer's instructions. Multiplex PCR was done to amplify five RDs, which were RD1, RD2, RD14 (RD8 according to the nomenclature of Bedwell et al. [5]), RD15 and RD16, as well as SenX3-RegX3. The sequences of the primers, the cycling profiles, and other conditions were the same as reported by Bedwell et al. The primer set for RD1 was devised to reveal deletion by yielding a PCR product with a different size [5]. For amplification of RD16 alone, a different primer pair (ACATTGGGAAATCGCTGCTGTTG and GGCTGGTGTTTCGTCACTTC) to that used by Bedwell et al. [9] was employed to amplify a more restricted region of RD16 and increase the difference in size relative to the RD16 PCR product. PCR products were subjected to electrophoresis on 10–20% polyacrylamide gel and stained with ethydium bromide.

2.4. Sequencing of RD16 PCR products

The bands of the RD16 PCR products were cut out of the gel and sequenced with a DNA sequencer (ABI PRISM 310, Applied Biosystems Japan Ltd., Tokyo, Japan).

2.5. Tandem duplication PCR analysis

Junction regions resulting from tandem duplications (JDU) were analyzed by PCR using primers for JDU2A and JDU2B [7]. Because we could not obtain a clear PCR product for JDU2A using the primers described by Brosch et al. under our PCR conditions, we chose a modified primer pair for JDU2A (GGTCCACGGTCAGGTAATTG and GATGTCCAGCAGATCACCAA). The primer pair for JDU2B was TB3608.OF (GAACAGGGTCGCGGAGTCT) and TB3671.7R (GGGTTCATGAGGTGCTAGGG), as described by Brosch et al. [7].

2.6. Growth in mice organs

Six-week-old female C57BL/6 mice (Japan Charles River Inc, Yokohama, Japan) were intravenously injected with 10 μg (wet weight) of BCG grown to mid-log phase on Sauton's medium. Then the spleen, lungs, and liver were removed at various times, homogenized, and plated onto Middlebrook 7H10 agar medium. After 2–3 weeks, colonies were counted.

2.7. Statistical analysis

Statistical analyses were done using a Statview software (SAS Institute, Cary, NC, USA).

3. Results

3.1. Two types of colonies in Tokyo172

When BCG Tokyo172 preparations were cultured on Middlebrook 7H10 agar medium, two types of colonies with different shapes were observed (Fig. 1A). One was smooth, round, and dome-shaped in appearance (S-colony), while the other had a rough granular surface, and an irregular shape (R-colony). Both types were found in every Tokyo172 preparation examined, but S-colonies were always in the majority (over 90%). After several selections of each colony type, they were clearly separated into distinct types (Fig. 1B and C), implying that the bacilli forming S- and R-colonies were genetically different.

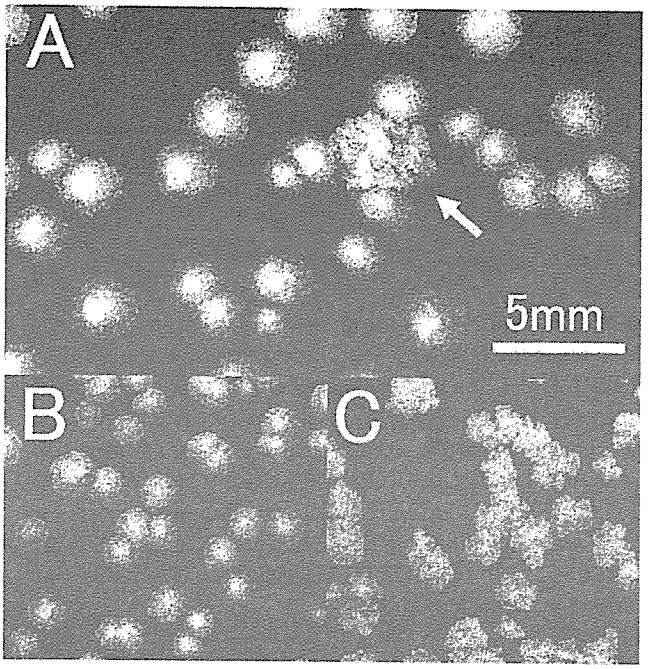

Fig. 1. Two types of colonies in BCG Tokyo172 substrain: (A) Tokyo172 preparation cultured on Middlebrook 7H10 agar medium for 4 weeks. Arrow indicates a R-colony surrounded by S-colonies; (B) isolated S-colonies; and (C) isolated R-colonies, each after single colony selections.

Fig. 2. (Top) Multiplex PCR analysis of the various BCG Tokyo172 specimens and BCG Birkhaug. FP, final product; SL, seed lot; SC, S-colony; RC, R-colony of BCG Tokyo172, respectively, and B, BCG Birkhaug. M, size marker. SX3-RX3, SenX3-RegX3. IRD1D, indicator of RD1 deletion. Arrows at RD16 indicate two types of PCR products differing in size; and (bottom) PCR analysis for the RD16 region showing the presence of type II genotype in BCG Tokyo172 preparations. The 22 bp sequence deleted from type I RD16 was used as one of the primer pair for RD16. AJ, ATCC BCG Japan; OSL, origin of seed lot; SL, seed lot; FP, final product; II, type II; I, type I; and M, size marker.

3.2. Two RD16 genotypes and relationship with colony morphology

When multiplex PCR was conducted on the Tokyo172 final product, seed lot, separate S- and R-colonies, and BCG Birkhaug, the patterns were almost indistinguishable from one another, except for slight differences of RD16 PCR product size-the R-colony and Birkhaug products were somewhat larger than the others on electrophoresis (Fig. 2 top). The genotype of Tokyo172 producing the smaller RD16 PCR product was defined as type I, and that producing the larger product was defined as type II. When PCR was done on each Tokyo172 colony formed on 7H10 medium, a strong relationship between colony morphology and genotype was shown, since 98.7% of S-colonies had the type I genotype and 95.9% of R-colonies had the type II genotype (Table 1). From these results, it was suggested that the Tokyo172 preparation mainly consisted of organisms with the type I genotype.

Sequencing of the type I and II RD16 PCR products showed a 22 bp deletion (GTGCAACAGTCTGGTCAGCTTC) in type I compared with type II. This sequence is a part of *Rv3405c* in RD16 (http://www.ncbi.nlm.nih.gov/blast/Blast.cgi). These results were exactly the same as Bedwell et al. reported for two genotypes found in a commercial Japanese preparation [5].

Table 1
Relationships between the colony morphology on Middlebrook 7H10 agar medium (S- or R-colony) and the RD16 genotype (type I or II) in BCG Tokyo172 preparation

	S-colonies ($n = 153$)	R-colonies ($n = 97$)
RD16 genotype		
I	151 (98.7%)	4 (4.1%)
II	2 (1.3%)	93 (95.9%)

To specifically detect type II genotype, PCR analysis was performed using the 22 bp sequence (GTGCAACAGTCTGGTCAGCTTC) deleted from the RD16 of type I, instead of one of the RD16 primer pair, to test ATCC BCG Japan, the origin of seed lot, the seed lot for production, the Tokyo172 final product, type I, and type II. In all cases except for type I, a band of the expected size (110 bp) was detected (Fig. 2 bottom), which indicated the presence of type II in all of the Tokyo172 preparations tested. However, the band for ATCC BCG Japan had a low density compared with others, suggesting a low content of type II in this preparation.

3.3. Difference in tandem duplication between Tokyo172 type II and BCG Birkhaug

The PCR patterns for JDU2A and JDU2B showed differences among BCG substrains, i.e., both the JDU2A and JDU2B bands in Pasteur, only the JDU2B band in Birkhaug, and no band in Tokyo172 (seed lot) or *M. tuberculosis* Aoyama B strain (the negative control). Both the type I and II of Tokyo172 also yielded no band (Fig. 3), which indicated

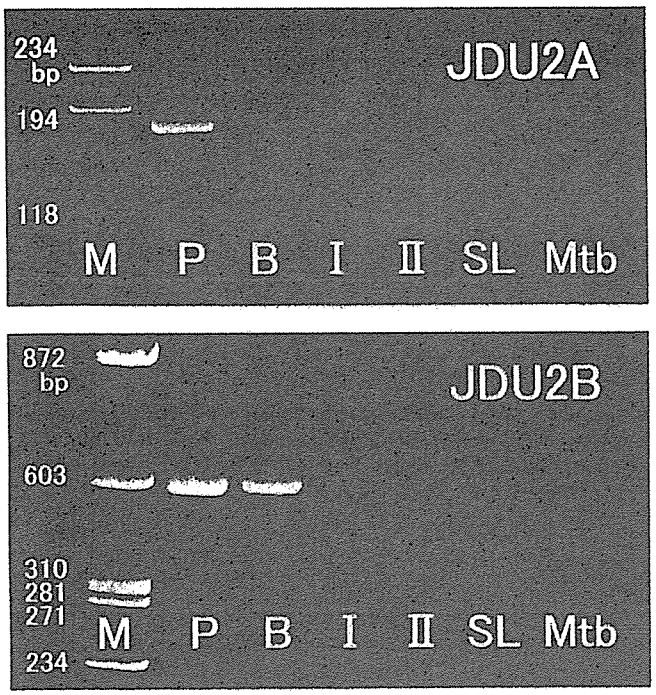

Fig. 3. Tandem duplication analysis by PCR on junction regions, showing distinct patterns between BCG substrains: (top) JDU2A and (bottom) JDU2B. P, BCG Pasteur; B, BCG Birkhaug; I, II and SL: type I, type II and seed lot of BCG Tokyo172, respectively; Mtb, *Mycobacterium tuberculosis* strain Aoyama B and M, size marker.

that DU2 mutations of these might exist in locations different from those of Birkhaug and Pasteur substrains.

3.4. Growth in mice organs

After 10 μg wet weight of the type I (4.6×10^5 CFU: colony forming units) or type II (3.7×10^5 CFU) was intravenously injected into C57BL/6 mice, the recovery of CFU from the spleen, lungs and liver was as shown in Fig. 4. In the spleen, type I increased at 2 weeks after injection to approximately five times the level at 1 day and gradually decreased

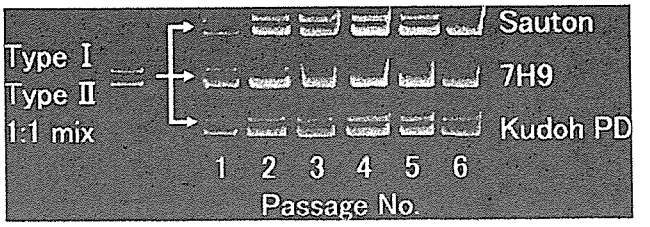

Fig. 5. Competition experiment on culture media showing a growth advantage of type I over type II. A mixture of equal amounts (by wet weight) of type I and type II was inoculated on Sauton's medium, Middlebrook 7H10 medium, or Kudoh PD egg slant medium, and thereafter serially passaged every 2 weeks, and PCR for RD16 was conducted.

thereafter, while type II did not increase much and stayed below type I throughout the experiment. In the lungs, both types did not show any apparent growth except for slight increase in type I at 4 weeks. Although the initial level of type II at 1 day was approximately six-fold higher than that of type I, it decreased rapidly. In the liver the tendency was similar as in the lungs; however, difference in initial level between both types at 1 day was not so apparent, and the increase of type I at 4 weeks was more pronounced, than in the case of the lungs. Difference between type I and type II was statistically significant in the spleen, but not in lungs and liver (Mann-Whitney's U-test, $p = 0.001$).

3.5. Growth competition studies in vitro and in vivo

When equal amounts (by wet weight) of type I and type II were mixed and inoculated on Sauton's medium, Middlebrook 7H9 medium, or Kudoh PD egg slant medium, and thereafter serially passaged every 2 weeks, the RD16 PCR analysis showed a decrease of type II compared with type I in every case. This occurred most rapidly in 7H9 medium, more slowly in Sauton's medium, and most gradually in Kudoh PD medium (Fig. 5). When 10 μg wet weight of the similar mixture of type I and type II (3.1×10^5 CFU) was injected intravenously into C57BL/6 mice, the type II/type I ratio (estimated from the recovered CFU numbers having S- or

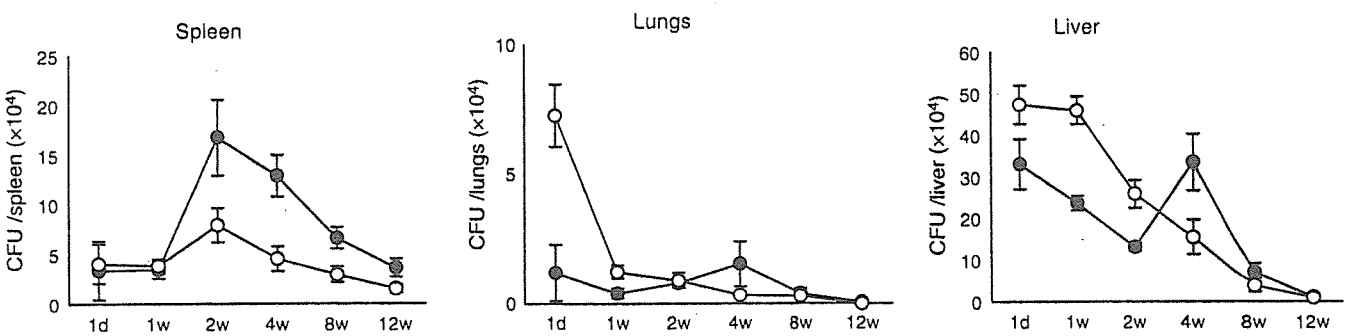

Fig. 4. Growth of type I and type II in mice organs. 10 μg wet weight of type I (4.6×10^5 CFU) or type II (3.7×10^5 CFU) was intravenously injected into C57BL/6 mice ($n = 3$), and CFU recovered from the spleen, lungs and liver from 1 day to 12 weeks after injection, were counted. Closed circles: type I, open circles: type II. Error bars: standard deviations. Difference between type I and type II was significant in the spleen (Mann-Whitney's U-test, $p = 0.001$), but not in lungs and liver.

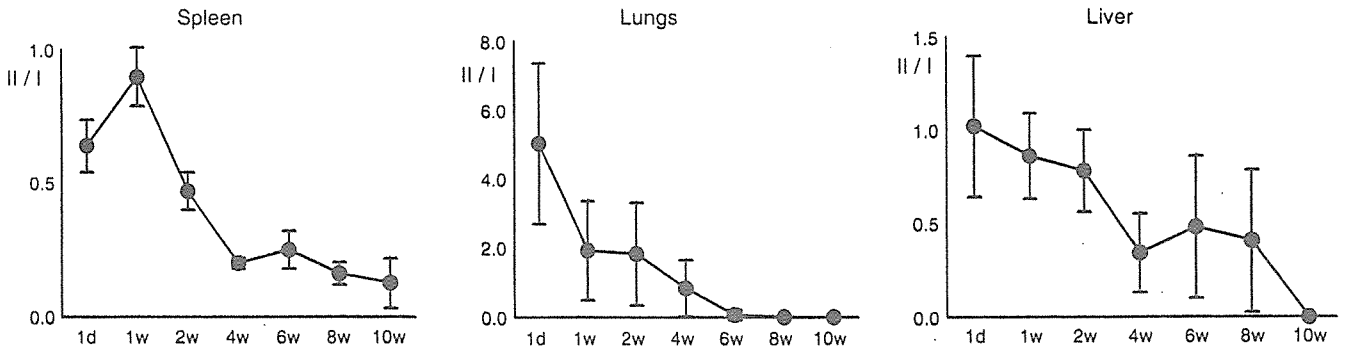

Fig. 6. Competition experiment in mice organs showing a growth advantage of type I over type II. A mixture of equal amounts of type I and type II (10 μg wet weight, 3.1×10^5 CFU) was intravenously injected into C57BL/6 mice ($n = 5$), and the changes of the type II/type I ratio in the spleen, lungs and liver from 1 day to 10 weeks after injection were investigated. Type II/type I ratio was estimated from the recovered CFU numbers having S- or R-colony morphology. Error bars: standard deviations.

R-colony morphology) in the spleen, lungs and liver showed a tendency to decrease over time in every case (Fig. 6).

4. Discussion

In BCG Tokyo172 substrain, the two colony morphologies (smooth: S and rough: R) were strongly related to the two genotypes, i.e., type I with a 22 bp deletion in *Rv3405c* of RD16, and type II without the deletion, similar to many other BCG substrains. As far as we know, this is the first time that a relationship between colony morphology and genotype in BCG has been identified. Type II likely corresponds to the genotype which Bedwell et al observed, and speculated might involve contamination of BCG Tokyo with another substrain [5]. Since they also found that this genotype had an identical multiplex PCR pattern to that of BCG Birkhaug, we conducted experiments to determine if type II is different from BCG Birkhaug or not. As a result, it was newly found that type II gave different results from BCG Birkhaug on DU2 in tandem duplication analysis. This is the first time in which tandem duplications were analyzed and compared between BCG substrains by PCR, and the results suggested a possibility for distinguishing BCG substrains by this method. IS6110 RFLP of types I and II produced two bands (unpublished data), similar to the results reported for Tokyo172 [10], while the Birkhaug substrain is known to show a single band [11]. Accordingly, type II was considered to be genetically different from BCG Birkhaug. Type II was present in every Tokyo172 preparation studied including the seed lot, the origin of seed lot, and ATCC BCG Japan. Also, the RD regions (including RD16) and SenX3-RegX3 of types I and II were stable after 20 serial passages in three types of media (same as those used in growth competition experiment, data not shown), indicating that transition from type II to type I is unlikely. Altogether, it was suggested that types I and II represented different genotypes, each constituting different subpopulations within the Tokyo172 substrain, and that this was not caused by the contamination of another BCG substrain. Since the proportion of type II seemed lower in ATCC BCG Japan than in other Tokyo172 preparations, and the sensitivity of multiplex PCR for minor components is not high, it is not surprising that Bedwell et al. could not find a type without the 22 bp deletion in RD16 region (type II) in ATCC BCG Japan.

An association between colony morphology and RD16 genotype was implied in this study, which raises the possibility of using colony morphology as a substitute for RD16 genotyping of Tokyo172 preparations. The morphology of BCG colonies is suggested to be related to cell wall components such as mycoside B [12], and a deletion in *Rv3405c*, which codes for a possible transcriptional regulatory protein (Tuberculist, http://genolist.pasteur.fr/TubercuList/) of which the function is not yet clear, might affect their synthesis or metabolism through some ways. However, rare exceptions did exist, i.e., some R-colonies had a type I genotype, and some S-colonies had a type II genotype. This might indicate the existence of factors other than the deletion in *Rv3405c* of RD16, which influence colony morphology. It is not clear if these exceptions are distinct genotypes within types I or II, or caused by changes in the expressions of some genes outside *Rv3405c*. The fact that BCG Moreau, which has a complete deletion of RD16, showed a rough colony morphology similar to type II when grown on 7H10 medium (data not shown) also suggests the existence of more complicated mechanisms.

In every Tokyo172 preparation studied, S-colonies exceeded 90% of the total. Accordingly, it is probable that the Tokyo172 preparation is mainly comprised of type I genotype, and that the known characteristics of this preparation, such as high viability and good heat stability [13], are those of type I bacilli. Type I probably arose from type II by mutation after delivery of BCG to Japan in 1924, since a similar deletion in RD16 has not been found in other BCG substrains so far [5,9]. From its relative abundance, type I is considered to correspond to the 'spreading colonies' which Osborn have reported [4] (and probably type II corresponds to the 'non-spreading colonies'), but difference in colony spread was not apparent on Middlebrook 7H10 agar. Type I seemed to have

growth advantage over type II both on culture media and in mice organs, and the former in vitro tendency might be one of the reasons why type I was always the major component of the Tokyo172 preparations. Judging from the present results, the 22 bp deletion in *Rv3405c* did not seem to affect growth in vitro or in vivo. It is not known if this deletion does not affect the growth of type I because *Rv3405c* is not expressed/functional, or if there exists some unknown difference between the genotypes of types I and II, which compensates for the drawback of this deletion and further favors growth of type I. Preliminary experiments have indicated that immunogenicity, which is believed to be related to the replication of BCG in the host [13], also seemed to be greater for type I than type II, as determined from IFN-γ secretion by sensitized spleen cells (data not shown). However, early preferential accumulation of type II (at 1 day) in the lungs (and also to some extent in liver) was observed, although it was cleared rapidly thereafter. The reason for this, and whether this has any consequences on the host responses, are not clear. Deletion in *Rv3405c* might be influencing on this phenomenon, through some changes in surface molecules of the bacilli. In the clinical setting, multiplex PCR investigation of specimens from patients receiving BCG vaccination or BCG therapy for bladder cancer have shown that only the genotype with deletion in RD16 (type I) was recovered in every case [9], results which coincide with the present competition study in mice. These results together with the suggested lower virulence of type II from histopathological studies run in parallel (data not shown), indicate that co-existence of a small amount of type II in the Tokyo172 preparation is unlikely to be problematic by affecting its immunogenicity and safety, although further investigations including protection against virulent *M. tuberculosis* or growth in immunocompromised animals, still need to be continued.

Tokyo172 (BCG Japan) is known to be one of the three substrains (Japan, Moreau, and Russia) with the fewest genetic mutations [8]. Among them, Japan had smallest deletion [14], and this remains true even when the 22 bp deletion of RD16 is included. Moreover, the type II bacilli of Tokyo172 (lacking the deletion in RD16) might be one of the BCG which most inherited the genotypes of the Calmette and Guérin's original BCG.

Since BCG was not established as a clone, it might be natural that BCG originally consisted of multiple subpopulations with different genotypes, and this characteristic is still maintained by many established BCG substrains including Tokyo172. The same investigations for other BCG substrains will undoubtedly benefit to ensure the safety and reliability of BCG as a tuberculosis vaccine or a therapeutic agent for bladder cancer.

References

[1] Petroff SA, Branch A, Steenken Jr W. A study of bacillus Calmette-Guérin (BCG). I. Biological characteristics, cultural "dissociation" and animal experimentation. Am Rev Tuberc 1929;19:9–46.
[2] Behner DM. The stability of the colony morphology and pathogenicity of BCG. Am Rev Tuberc 1935;31:174–202.
[3] Pierce CH, Dubos RJ. Differential characteristics in vitro and in vivo of several substrains of BCG. II. Morphologic characteristics in vitro and in vivo. Am Rev Tuberc Pulm Dis 1956;74(5):667–82.
[4] Osborn TW. BCG vaccine: an investigation of colony morphology from four different strains after their introduction as seed for vaccine preparation in four production laboratories. J Biol Stand 1983;11:19–27.
[5] Bedwell J, Kairo SK, Behr MA, Bygraves JA. Identification of substrains of BCG vaccine using multiplex PCR. Vaccine 2001;19:2146–51.
[6] Behr MA, Wilson MA, Gill WP, Salamon H, Schoolnik GK, Rane S, et al. Comparative genomics of BCG vaccines by whole-genome DNA microarray. Science 1999;284:1520–3.
[7] Brosch R, Gordon SV, Buchrieser C, Pym AS, Garnier T, Cole ST. Comparative genomics uncovers large tandem chromosomal duplications in *Mycobacterium bovis* BCG Pasteur. Yeast 2000;17:111–23.
[8] Behr MA. Comparative genomics of BCG vaccines. Tuberculosis 2001;81:165–8.
[9] Seki M, Sato A, Honda I, Yamazaki T, Yano I, Koyama A, et al. Modified multiplex PCR for identification of Bacillus Calmette-Guérin substrain Tokyo among clinical isolates. Vaccine 2005;23:3099–102.
[10] Fomukong NG, Dale JW, Osborn TW, Grange JM. Use of gene probes based on the insertion sequence IS986 to differentiate between BCG vaccine strains. J Appl Bacteriol 1992;72:126–33.
[11] Behr MA. BCG-different strains, different vaccines? Lancet Infect Dis 2002;2:86–92.
[12] Abou-Zeid C, Rook GAW, Minnikin DE, Parlett JH, Osborn TW, Grange JM. Effect of the method of preparation of Bacille Calmette-Guérin (BCG) vaccine on the properties of four daughter strains. J Appl Bacteriol 1987;63:449–53.
[13] Gheorghiu M, Lagrange PH. Viability, heat stability and immunogenicity of four BCG vaccines prepared from four different BCG strains. Ann Immunol (Inst Pasteur) 1983;134C:125–47.
[14] Mostowy S, Tsolaki AG, Small PM, Behr MA. The in vitro evolution of BCG vaccines. Vaccine 2003;21:4270–4.

Available online at www.sciencedirect.com
SCIENCE DIRECT
ELSEVIER
Microbial Pathogenesis 40 (2006) 245–253
MICROBIAL PATHOGENESIS
www.elsevier.com/locate/micpath

Mycobacterial sulfolipid shows a virulence by inhibiting cord factor induced granuloma formation and TNF-α release

Yuko Okamoto [a], Yukiko Fujita [a,*], Takashi Naka [a], Manabu Hirai [b], Ikuko Tomiyasu [c], Ikuya Yano [a]

[a] *Japan BCG Central Laboratory, 3-1-5 Matsuyama, Kiyose-shi, Tokyo 204-0022, Japan*
[b] *Osaka City University Medical School, 1-4-3 Asahi-machi, Abeno-ku, Osaka 545-8586, Japan*
[c] *Tezukayama University, 7-1-1 Tezukayama, Nara-shi, Nara 631-8501, Japan*

Received 18 October 2005; accepted 10 February 2006
Available online 19 April 2006

Abstract

Virulence mechanism of infection with *Mycobacterium tuberculosis* is currently focused to be clarified in the context of cell surface lipid molecule. Comparing two mycobacterial glycolipids, we observed toxicity and prominent granulomatogenic activity of trehalose 6,6′-dimycolate (TDM) injection in mice, evident by delayed body weight gain and histological observations, whereas 2,3,6,6′-tetraacyl trehalose 2′-sulfate (SL) was non-toxic and non-granulomatogenic. Likewise, TDM but not SL caused temporarily, but marked increase of lung indices, indicative of massive granuloma formation. Interestingly, co-administration of TDM and SL prevented these symptoms distinctively and SL inhibited TDM-induced release of tumor necrosis factor alpha (TNF-α) in a dose-dependent manner. Histological findings and organ index changes also showed marked inhibition of TDM induced granuloma formation by co-administration of SL. Simultaneous injection of SL together with TDM was highly effective for this protection, as neither injection 1 h before nor after TDM injection showed highly inhibitory. In parallel studies on a cellular level, TDM elicited strong TNF-α release from alveolar but not from peritoneal macrophages in vitro. This effect was blocked when alveolar macrophages were incubated in wells simultaneously coated with TDM and SL, indicating that SL suppresses TDM-induced TNF-α release from macrophages. Our results suggest a novel mechanism by which SL could contribute to virulence at early stage of mycobacterial infection or stimulation with the glycolipids by counteracting the immunopotentiating effect of TDM.

Keywords: *Mycobacterium tuberculosis*; Trehalose dimycolate; Cord factor; Sulfolipid; Tumor necrosis factor alpha; Granuloma formation

1. Introduction

Cord factor (trehalose 6,6′-dimycolate, TDM) and sulfolipid (2,3,6,6′-tetraacyl trehalose 2′-sulfate, SL; Sulfatide-1, SL-1) are well-known glycolipids of *Mycobacterium tuberculosis* [1–3], as shown in Fig. 1. Thin-layer chromatographic analysis of glycolipids for *M. tuberculosis* Aoyama B showed two distinctive spots corresponding to TDM and SL (Fig. 2). Both glycolipids, SL and TDM possess trehalose and branched chain fatty acids, namely phthioceranic or hydroxy phthioceranic acid for SL and mycolic acid for TDM. A difference between SL and TDM is the occurrence of sulfate group in the trehalose moiety of SL, but not of TDM. So, SL is a characteristic anionic glycolipid, while TDM is a neutral glycolipid, respectively.

SL has long been reported to be correlated with virulence [4,5], and the virulence mechanism has been proposed to include inhibition of phagosome–lysosome fusion [6], suppression of priming for enhanced release of superoxide by lipopolysaccharide (LPS), IFN-γ, interleukin-1β and TNF-α [7,8], and self-damage of phagocytes by the release of superoxide [9]. On the other hand, since association of strains showing cord like growth with virulence has been recognized early in the history of mycobacterial research [10], TDM, the principle molecule for cord-formation, subsequently has shown the both edges of the sword such as granulomatogenicity [11–14], induction activity of chemotactic factors [15–18], anti-tumor activity [19–21], Th-1 type immuno adjuvant activity [16,17,20,22,23], inducibility of thymic atrophy [24,25] and lethal toxicity [15,26–28]. However to date, the virulence mechanism related to the both glycolipids has not been elucidated, although the structure resembles each other in possessing acyl trehalose moiety.

* Corresponding author. Tel.: +81 424 91 0611; fax: +81 424 92 9752.
E-mail address: y-fujita@bcg.gr.jp (Y. Fujita).

0882-4010/$ - see front matter © 2006 Elsevier Ltd. All rights reserved.
doi:10.1016/j.micpath.2006.02.002

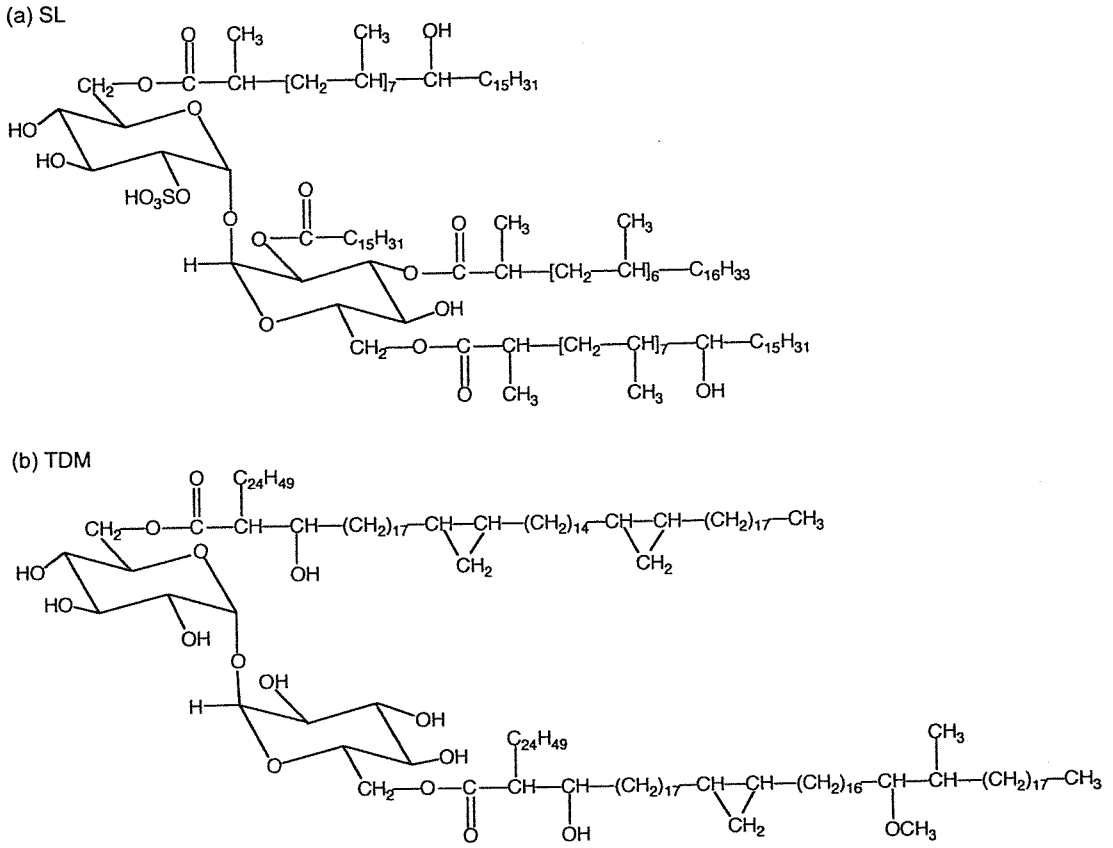

Fig. 1. Structure of SL and TDM from *M. tuberculosis* Aoyama B. (a) SL contained one molecule of palmitic, phthioceranic and two molecules of hydroxy phthioceranic acid ranging from C_{36} to C_{46}, and the total mass number ranged from *m/z* 2100 to 2750. (b) TDM contained two molecules of mycolic acids from any of alpha-, methoxy- or keto-mycolic acid with the carbon chains ranging from C_{76} to C_{92}, and the total mass number ranged from *m/z* 2600 to 3000.

Recently, there have been reported that highly transmissible *M. tuberculosis* strains inducible vigorous host responses are not necessarily highly virulent [29–31], and suggested that certain *M. tuberculosis* strain with high pathogenicity produce lipids that fail to efficiently induce the cytokine dependent Th-1 type protective immune response [32]. We have intended to reveal whether SL may affect directly or indirectly to the host immune response as a virulence factor of highly pathogenic strain of *M. tuberculosis*. Consequently, the presence of TDM alerts the immune system and therefore might be detrimental to mycobacterial survival in the host, while SL seems to be a specific virulence factor which suppresses the host protective activity of TDM.

2. Results

2.1. Toxicity and granuloma forming activity of TDM and SL

We first examined the time course changes in body weight for evaluating the toxicities of TDM and SL after i.v. injection in w/o/w-emulsions of each glycolipid or vehicle controls. Body weights were comparable on day 1 in all groups. By day 7 a clear increase was observed in control and SL injected groups (Fig. 3(a)). In contrast, the values of mice which had received injections of TDM were not increased as all animals suffered from peritonitis and concomitant diarrhoea. At the last

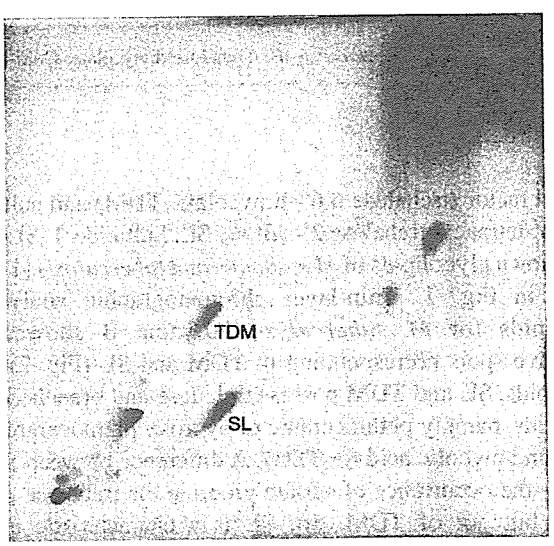

Fig. 2. Two-dimensional thin-layer chromatogram of glycolipids from *M. tuberculosis* Aoyama B. Total extractable lipids (100 μg) were developed with chloroform/methanol/water (90:10:1, by vol.; first dimension, upper) and chloroform/methanol/acetone/acetic acid (90:10:6:1, by vol.; second dimension, horizontal). Glycolipid spots were visualized with a 9 M H_2SO_4 spray followed by charring at 200 °C. Relative amount of SL to TDM was shown to be approximately same or little higher.

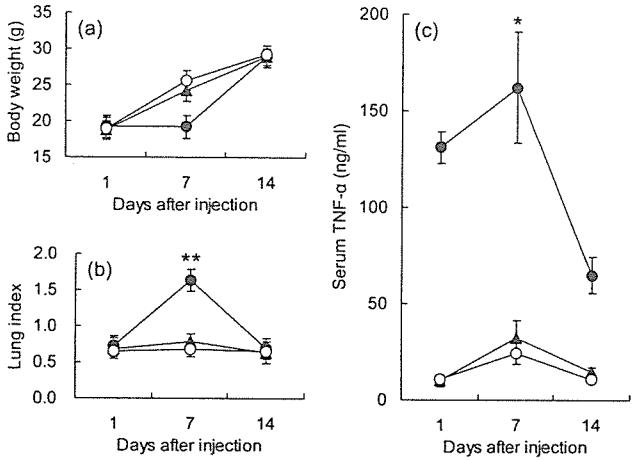

Fig. 3. Time course changes in body weight, lung index and serum TNF-α level after i.v. injection of TDM or SL. Mice received an i.v. injection of 300 μg TDM (closed circles ●), SL (triangles ▲) or the w/o/w-vehicle (open circles ○). Body and organ weights and serum TNF-α level were estimated on the indicated days. (a) Body weights; (b) lung indices; lung index of mouse injected with TDM on day 7 was significantly increased compared with that of SL injected mouse (**$P<0.01$); (c) serum TNF-α level; TNF-α level in mouse sera after priming with TDM and eliciting with LPS was significantly higher than that after priming with SL and eliciting with LPS (*$P<0.05$).

measurement at day 14, SL injected and control groups had additionally increased their body weights, while TDM injected group had overcome the toxic effects of this substance and also had a body weight comparable to that of the other groups. On day 7, TDM caused a marked increase in lung index compared to a slight increase in SL injected group (Fig. 3(b)). By day 14, the indices of both groups had returned to that of the control group. To correlate both the observed toxic effect of TDM and granuloma formation with a potential mediator, we measured TNF-α release in TDM- or SL-primed mice before triggering with LPS. Serum TNF-α concentration of SL-primed group were indistinguishable from those of control group, whereas a marked elevation was observed on day 7 after injection in TDM-primed group (Fig. 3(c)).

2.2. Histological findings on the antagonistic effect of SL upon the TDM-induced granuloma formation

As shown in above data, TDM and SL exhibited different biological activities in granulomatogenic responses, despite of the similar structure, we co-administered the both TDM and SL. Lung granuloma formation with i.v. injection of TDM was clearly dose responsive up to 300 μg/mouse. Histologically, i.v. injection of 300 μg TDM generated multiple massive granulomas widely in the both lung lobes with a marked infiltration of mature or immature macrophages and lymphocytes, and the heavily thickening of the alveolar interstitial tissues was observed (Fig. 4(c)). Co-administration of 300 μg TDM and 100 μg SL showed a slight inhibition of TDM-induced cellular infiltration, especially of macrophages and the resultant suppression of granuloma formation (Fig. 4(d)). Interestingly, co-administration of each 300 μg TDM and 300 μg SL showed a dramatical inhibition for granulomatous infiltration in lungs of mice near to the vehicle control level (Fig. 4(e)). However, single injection of SL did not show any massive granulomatous changes in lungs (Fig. 4(b)). Notably, for the highest inhibition with SL on TDM-induced granuloma formation simultaneous administration of the both glycolipids was essential (Fig. 4(e)), and SL injection at one hour before and after TDM injection lost the highly inhibitory effect of SL (Fig. 4(f)). These inhibitory effect of SL on TDM-induced granuloma formation in vivo was confirmed by lung and splenic index changes, as shown in Fig. 5(a) and (b). In both organs, increases in organ indices with 300 μg TDM injection were clearly inhibited by co-administration of 300 μg SL.

2.3. Paralleled inhibition of TDM-induced granuloma formation and TNF-α release by SL in vivo

Further interest is the inhibitory effect of SL on the TDM-induced granuloma formation and TNF-α release in mice. Addressing this issue in a more detailed experimental setting, we indeed confirmed that the presence of SL inhibited TDM-induced TNF-α release clearly in a dose-dependent manner (Fig. 6(a)). In parallel to the inhibition of TNF-α generation by SL, lung indices declined with increasing amounts of SL, and in mouse system co-administrated with 300 μg TDM and 300 μg SL the observed reduction was statistically significant (Fig. 6(b)). In additional experiments, we studied the time-dependency of the antagonistic effect of SL and found that simultaneous administration with the both glycolipids was necessary (Fig. 5). Injection of SL one hour before or after TDM injection was not sufficient to rescue mice from TDM-induced effects (subsequent loss or delayed gain of body weight, increase of lung index and high TNF-α levels).

2.4. TNF-α release by macrophages from ICR mice in response to TDM in vitro

To investigate the mechanism of the in vivo effects of SL on a cellular level, we first determined the release of TNF-α by alveolar macrophages (AM) and peritoneal macrophages (PM) with TDM stimulation. Harvesting culture supernatants after 24 h, we found highly elevated levels of TNF-α after incubation of AM in wells coated with various amounts of TDM in the range between 0 and 20 μg/well (Fig. 7(a)). In supernatants collected after 72 h also TNF-α concentrations in wells with 0.8 and 4.0 μg TDM showed clear increases from the background levels. Clear dose response curves were observed with TDM concentration between 0.032 and 0.8 μg in both cases of 24 and 72 h incubation of AM, although TNF-α concentration in the supernatant from PM was lower (Fig. 7(b)).

2.5. Antagonistic effect of SL on TDM-induced TNF-α release by macrophages from ICR mice in vitro

To model the in vivo TDM and SL co-administration experiments, the studies were carried out in the wells coated with both TDM and SL (Fig. 8(a)). AM were used because in

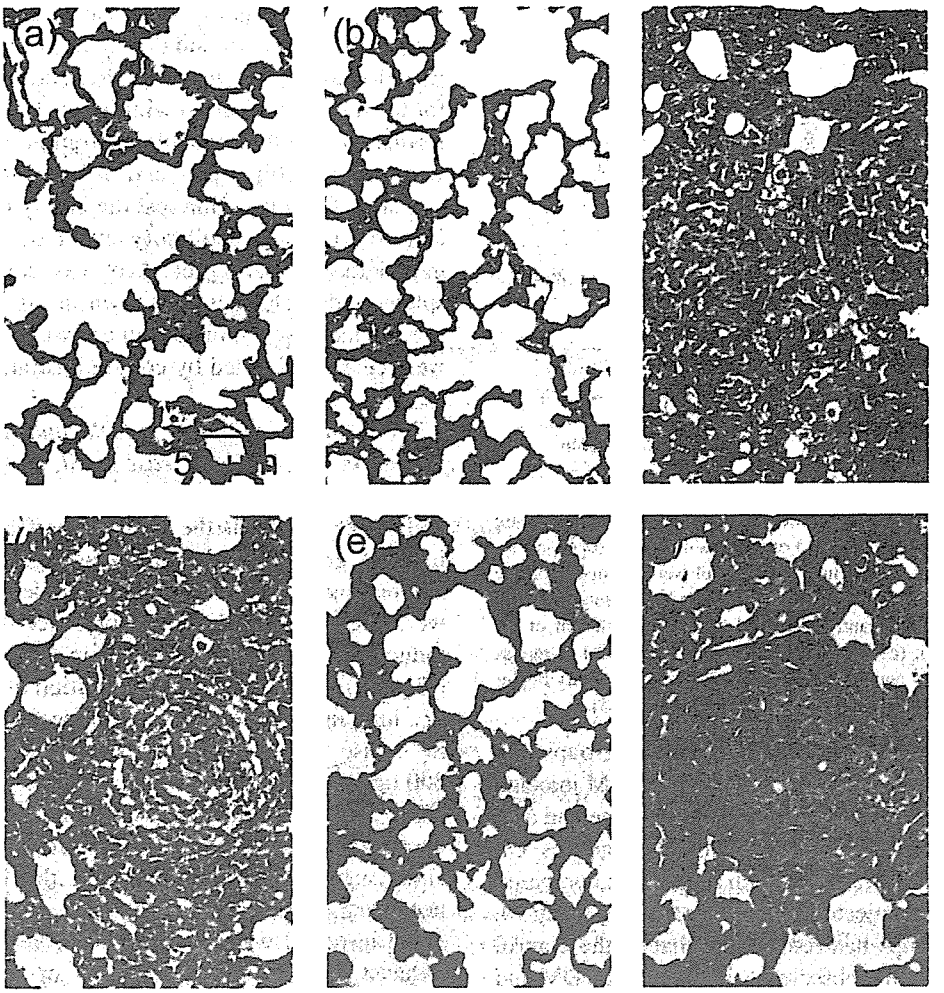

Fig. 4. Histological observation of lung granuloma formation by single or co-administration of TDM and/or SL in mice (H-E stain). (a) Control; (b) SL (300 μg/mouse); (c) TDM (300 μg/mouse); (d) TDM + SL (simultaneous co-administration of both TDM (300 μg/mouse) and SL (100 μg/mouse)); (e) TDM + SL (simultaneous co-administration of both TDM (300 μg/mouse) and SL (300 μg/mouse)); (f) TDM → SL (SL (300 μg/mouse) was injected 1 h after injection of TDM (300 μg/mouse)). Magnification, ×200.

contrast to PM they had been exposed and stimulated with the external foreign antigens and clearly TDM-responsive, thereby probably reflecting the importance of lung as entry site of *M. tuberculosis*, main target organ and consequently primary site of the defense. As maximum TDM-dependent TNF-α release had been observed in the wells coated with 0.8 μg TDM in the preceding experiment (Fig. 7(a)), this fixed value was tested together with increasing amounts of SL. In the range of 0.8–20 μg SL/well TNF-α production was reduced in a clearly dose-dependent way until maximum inhibition occurred at 4.0 μg (Fig. 8(a)).

2.6. Strain specificity of the antagonistic effect of SL

To determine if the observed effect of SL on TNF-α release depends on the genetic background of mice, the in vitro experiments were carried out with AM isolated from ICR, BALB/c and C3H/HeN mice, each of which differed in the sensitivity of granulomatogenicity to TDM, as reported previously [33]. Co-incubation with 0.8 μg TDM and 4.0 μg SL showed marked decreases in TNF-α release than incubation with 0.8 μg TDM solely in all cases (Fig. 8(b)). Since, all the mouse strains showed the similar tendencies in SL inhibition to TDM dependent TNF-α release in vitro, we concluded that the underlying mechanism is independent from the genetic factors which determine the susceptibility of the mouse strains to TDM-induced granuloma formation.

3. Discussion

Mycobacterial cell wall components have been shown to affect the immune response by modulating diverse cytokine patterns [34–36]. Among such components, TDM and SL, both being major components and having acyl trehalose moiety, have been focused from the aspect of virulence-associated factors. However, TDM has been recognized to be ubiquitous component distributed widely among pathogenic and non-pathogenic mycobacteria, while SL to be detected in only virulent strains isolated from human specimens [5,37–39]. Therefore, we have postulated that the structure and virulence activity relationship may be critically important. Studying on TDM-induced hypersensitivity to endotoxin shock, we

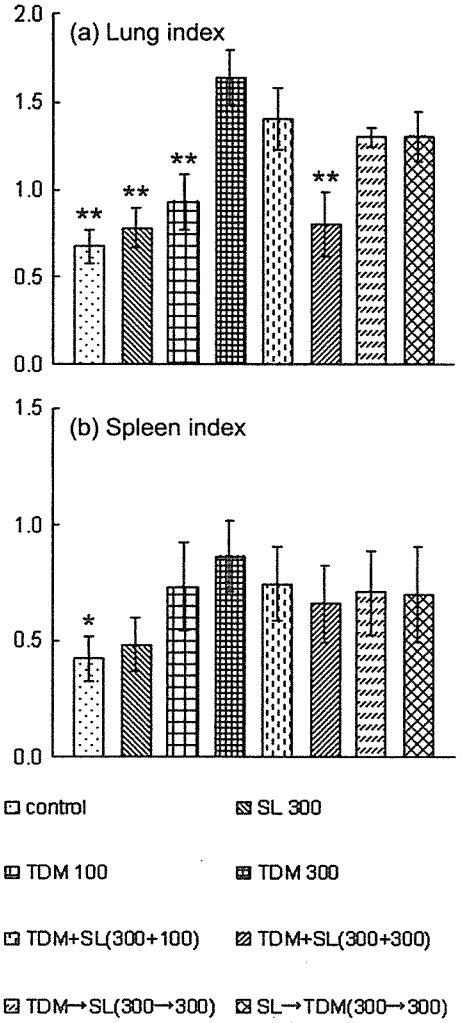

Fig. 5. Inhibition of TDM-induced granuloma formation by co-administration of SL assessed by lung or splenic indices in mice. Body and organ weights were estimated on day 7 after injection of glycolipids, and then lung and spleen indices were calculated. The asterisks *, indicate a P-value of <0.05 and **, indicate a P-value of <0.01 compared to 300 μg TDM injected mice.

previously obtained indications that SL might directly antagonize certain TDM effects [40]. In our present study, we therefore investigated the combined effect of TDM and SL on the granuloma formation and TNF-α release in mice. In vivo experiments demonstrated that the increase in TNF-α release and concomitantly higher granulomatous changes or lung indices after TDM injection. SL acted neutrally when delivered individually, but antagonistically by co-administration with TDM, and consequently decreased TNF-α levels and reduced lung indices towards normal values. Likewise, in vitro studies presented a coherent picture fitting to the in vivo results. AM responded well to TDM for TNF-α production, thus providing one explanation for the particular propensity of this organ for TDM-induced granuloma formation. SL, which by itself did not cause release of TNF-α, clearly blocked the induction of this cytokine with TDM in in vitro experiments.

The importance of TNF-α in host defense mechanism against mycobacterial infection has been vigorously investigated, and the reduction of granuloma formation and bactericidal mechanism and alteration of the mycobacterium-induced Th-1 type immune response have been reported in TNF-α blocked mice [41–46]. It is also known that blocking of TNF-α by anti-TNF-α antibodies resulted in rapid death of infected mice, delayed production of bactericidal nitric oxide and impaired containment of bacteria in granulomas [43]. By antagonizing TNF-α release, mycobacteria would therefore ensure a more hospitable environment. The potential clinical significance of our results becomes clear in the context of observations made by various groups in the past years: Flynn et al. demonstrated continuous expression of TNF-α during quiescent infection [47], and Adams et al. showed that neutralization of TNF-α by over expression of the extracellular domain of the TNF-α receptor exacerbated both acute and chronic infection [48]. Recently, a detailed study about the effects of TNF-α neutralization during latent tuberculosis revealed numerous histological changes including disorganization of granulomas, diffuse infiltration of inflammatory cells and increased apoptosis [49]. Considering the obvious importance of TNF-α for properly organized granulomas and

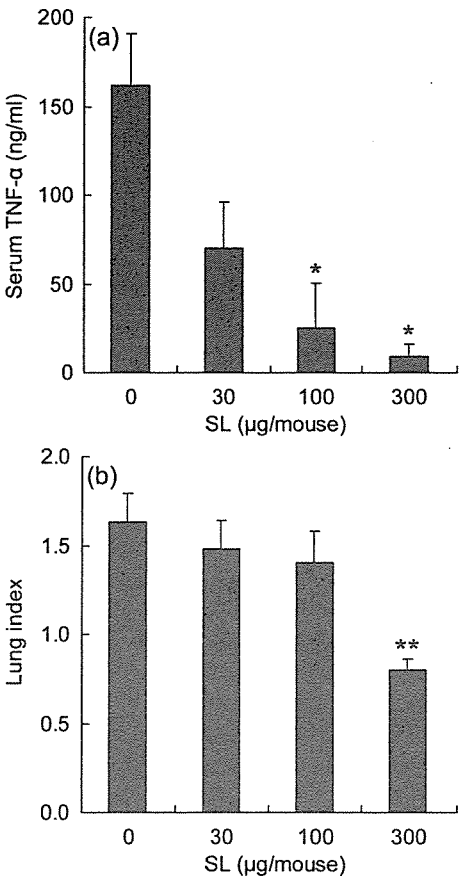

Fig. 6. Dose responsive inhibition of serum TNF-α induction and TDM-induced granuloma formation by SL. Mice were received co-administration of 300 μg TDM and 0, 30, 100 or 300 μg SL intravenously in w/o/w micelles. (a) Serum TNF-α release was triggered by i.v. injection of 100 μg LPS on day 7 post injection of TDM with or without of SL and sera were taken 2 h later. The asterisks *, indicate a P-value of <0.05 compared to 300 μg TDM injected mice. (b) On day 7 body and organ weights of all mice were measured for determination of lung indices. The asterisk **, indicate a P-value of <0.01 compared to 300 μg TDM injected mice.

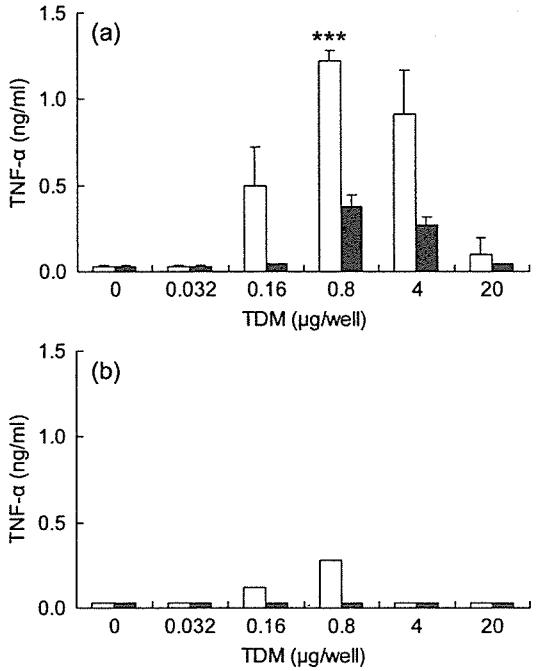

Fig. 7. In vitro effect of TDM on serum TNF-α production in alveolar or peritoneal macrophages in mice (a) and (b); wells were coated with the indicated amounts of TDM and the solvent was dried up completely. AM (a) or PM (b) (5.0×10^5 cells) were added in each well. After 24 h (white bars) or 72 h (black bars) supernatants were collected and assayed for TNF-α. TDM-induced TNF-α production by AM was significantly higher than that from PM (***$P<0.001$).

thus for containment as prerequisite for effective suppression of mycobacteria, the potential significance of a TNF-α-blocking mechanism for *M. tuberculosis* is evident. In view of these data it is interesting that already decades ago Gangadharam et al. linked the virulence of Indian and British strains of *M. tuberculosis* to their SL content [4,5]. They showed highly virulent strain of *M. tuberculosis* human isolates contained higher amount of acidic glycolipids, and later the conclusion was confirmed by Goren et al. after application of more stringent methods for the isolation of SL [37].

SL was initially isolated from the virulent laboratory strain *M. tuberculosis* $H_{37}Rv$ but absent from the avirulent strain *M. tuberculosis* $H_{37}Ra$ [50]. Since then, the most highly virulent strain of *M. tuberculosis* have been reported generally to produce SL. In such virulent strains of *M. tuberculosis*, relative amount of SL to TDM is around comparable or higher than that of TDM (Fig. 2) and SL is more unstable than TDM [3], and in the administration study, most of investigators used 100–300 μg TDM in w/o/w micelles intravenously in mice for granuloma formation model [11–14]. We do not necessarily require such large amount of glycolipids for the experimental study, but we considered that these amounts of administration give the most reliable results. Initially, we have expected that SL may have a direct inhibitory effect against granulomatous response and TNF-α release, however, after co-administration, SL inhibited these responses indirectly via the TDM stimulation in vivo and in vitro. Thus, taken together, the suppression of TDM-induced TNF-α production and the inhibition of granuloma formation might constitute a new virulence function for SL.

Recently, Rousseau et al. showed that SL deficiency dose not significantly affect the replication, persistence and pathogenicity of *M. tuberculosis* $H_{37}Rv$ in mice and guinea pigs or in cultured macrophages, using a *pks* 2 knockout strain of *M. tuberculosis* $H_{37}Rv$ [51]. This mutant strain lacked the synthesis of phthioceranic and hydroxyl phthioceranic acids and consequently lacked SL, and further possibly devoided of the virulence attenuation factors [52]. One reason of the difference between two set of pairs; $H_{37}Rv$ and $H_{37}Ra$ or $H_{37}Rv$ (wild) and $H_{37}Rv$ *pks* 2 is that virulence is a complex phenotypic trait, and it may be possible that other factors in the *M. tuberculosis* $H_{37}Rv$ SL-deficient mutant compensate for the lack of SL. Therefore, further studies on the virulence analysis of recent clinical isolates will be necessary to clarify the role of SL.

The mechanism for inhibitory effect of SL on TDM-induced granuloma formation and TNF-α induction is not entirely known at the present stage. However, since the present study showed that the structure similarity of the both glycolipids existed distinctively, the simultaneous administration of TDM and SL to mice was necessary for the inhibitory effect, and the paralleled inhibition was observed by SL of TDM-induced TNF-α generation and granuloma formation in vivo and in vitro in dose dependent manner, there is a strong possibility

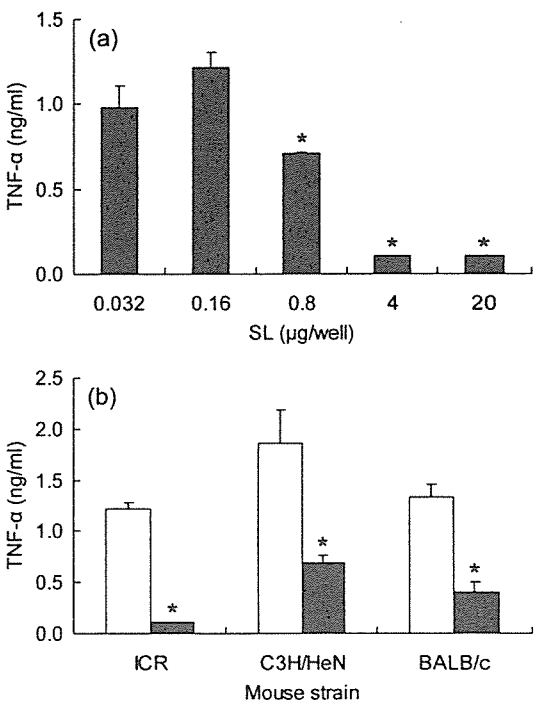

Fig. 8. In vitro effect of TDM and SL on serum TNF-α production in alveolar macrophages in mice. (a) AM were co-incubated in wells which contained 0.8 μg TDM and in addition the indicated amounts of SL. Supernatants were collected 24 h later and TNF-α concentrations were determined. The asterisk *, indicate a P-value of <0.05 compared to AM co-stimulated with 0.8 μg TDM and 0.032 μg SL. (b) AM were isolated from ICR, C3H/HeN and BALB/c mice and co-incubated in wells simultaneously coated with 0.8 μg TDM (white bars) or 0.8 μg TDM and 4.0 μg SL (black bars). Supernatants were collected after 24 h and assayed for TNF-α. In each strain of mice SL inhibited TDM-induced TNF-α production by AM (*$P<0.05$).

of a competitive inhibition of these two glycolipids against receptor binding site or macrophage activating step(s). In such context, identification of specific receptor(s) such as Toll-like receptor (TLR) or other signal transduction systems recently reported should be clarified in near future.

4. Materials and methods

4.1. Mice

Male BALB/c, C3H/HeN and ICR mice were purchased from Japan SLC Co., Shizuoka, Japan. All animals were 4-week-old at the start of the experiments and were kept under specific pathogen-free conditions.

4.2. Glycolipids

SL and TDM from *M. tuberculosis* Aoyama B were fractionated from the total extractable lipids, and were isolated and formulated as water/oil/water (w/o/w)-emulsions as described previously [40,53]. Total mass numbers of each SL and TDM were determined by matrix assisted laser desorption ionization-time of flight (MALDI-TOF) mass spectrometric analysis.

4.3. In vivo determination of TNF-α level after TDM and/or SL injection

For determination of serum TNF-α, ICR mice (five animals per group) were injected into the tail vein with 300 μg of TDM or SL as w/o/w-emulsions, and then stimulated on days 1, 7 or 14 by an intravenous injection of 100 μg *Salmonella minnesota* LPS (Difco Co.). Sera were collected 2 h later and TNF-α concentrations were determined in an assay using L929 cells as described elsewhere [54,55]. Quantitative results were derived from a calibration curve based on recombinant TNF-α (Genyzme).

For studying the effects of co-administration, ICR mice (five animals per group) were injected into the tail vein with 300 μg TDM together with 0, 30, 100 or 300 μg SL. After determination of body weights, stimulation with LPS on day 7 was performed as described above. Sera were taken 2 h later and lungs were removed for determination of lung indices.

4.4. Granuloma formation and determination of organ indices

ICR mice were injected into the tail vein with TDM and/or SL in w/o/w-emulsions or the vehicle control alone. On the indicated time points body weights and the weights of the isolated organs were determined. Organ indices were calculated according to the following formula: organ index is (organ weight/body weight) $\times 100$.

4.5. Histology

Samples from the lungs of mice 1 week after injection into the tail vein with TDM and/or SL in w/o/w-emulsions or the vehicle control alone were fixed with 10% formalin for 5 days, dehydrated, and embedded in paraffin. Sections were stained with hematoxylin and eosin.

4.6. Isolation of alveolar and peritoneal macrophages

For isolation of AM, 1 ml PBS was injected into the bronchus of each 5 ICR, C3H/HeN or BALB/c mice per group. After the thoracic cavities were opened, AM were collected by pumping and centrifugation at 1000 rpm for 10 min. The procedure was repeated 4–6 times and pooled washes were combined and centrifuged. Erythrocytes were lysed by incubation in Tris–NH_4Cl-buffer, and after the washed cells were resuspended in RPMI1640 supplemented with 10% FCS at a concentration of 5×10^6 cells/ml. A macrophage content of at least 90% was confirmed by methylene blue staining. For isolation of PM, 5 ICR mice per group received an intraperitoneal injection of 2.0 ml of 20% protease peptone. Four days later PM was harvested by flushing the peritoneal cavity twice with 5 ml PBS.

4.7. In vitro stimulation of alveolar and peritoneal macrophages for TNF-α production in TDM and/or SL coated wells

For studying the effect of stimulation of TDM in vitro, 50 μl hexane solution containing 0, 0.032, 0.16, 0.8, 4 or 20 μg TDM were added into wells of 96-well plates and kept in clean benches until the solvent was evaporated off. Similarly, for studying the effect of co-stimulation of TDM and SL, 50 μl hexane solution containing 0.8 μg TDM and 0.032, 0.16, 0.8, 4 or 20 μg SL were added into wells. 5×10^6AM or PM from ICR, C3H/HeN or BALB/c mice were added in a volume of 200 μl. After adhesion LPS was added at a final concentration of 1.6 μg/ml, cells were incubated at 37 °C for 24 or 72 h, and then culture supernatants were collected and stored at −80 °C until use.

4.8. Statistical analysis

Results are from $n=5$ mice and are from one representative experiment of three independent experiments of in vivo. Samples of in vitro cultures are from $n=5$ mice and are assayed in triplicate and represented a total of three independent experiments. The data represent the means ± SD. For statistical analysis the unpaired Student's *t*-test was used.

References

[1] Bloch H. Studies on the virulence of tubercle bacilli; isolation and biological properties of a constituent of virulent organisms. J Exp Med 1950;91:197–218.

[2] Noll H, Bloch H, Asselineau J, Lederer E. The chemical structure of the cord factor of *Mycobacterium tuberculosis*. Biochim Biophys Acta 1956; 20:299–309.

[3] Goren MB, Brokl O, Das BC. Sulfatides of *Mycobacterium tuberculosis*: the structure of the principal sulfatide (SL-I). Biochemistry 1976;15: 2728–35.

[4] Gangadharam PR, Cohn ML, Davis CL, Middlebrook G. Infectivity and pathogenicity of Indian and British strains of tubercle bacilli studied by aerogenic infection of guinea pigs. Am Rev Respir Dis 1963;87:200–5.
[5] Gangadharam PR, Cohn ML, Middlebrook G. Infectivity, pathogenicity and sulpholipid fraction of some Indian and British strains of tubercle bacilli. Tubercle 1963;44:452–5.
[6] Goren MB, D'Arcy Hart P, Young MR, Armstrong JA. Prevention of phagosome–lysosome fusion in cultured macrophages by sulfatides of *Mycobacterium tuberculosis*. Proc Natl Acad Sci USA 1976;73:2510–4.
[7] Brozna JP, Horan M, Rademacher JM, Pabst KM, Pabst MJ. Monocyte responses to sulfatide from *Mycobacterium tuberculosis*: inhibition of priming for enhanced release of superoxide, associated with increased secretion of interleukin-1 and tumor necrosis factor alpha, and altered protein phosphorylation. Infect Immun 1991;59:2542–8.
[8] Pabst MJ, Gross JM, Brozna JP, Goren MB. Inhibition of macrophage priming by sulfatide from *Mycobacterium tuberculosis*. J Immunol 1988; 140:634–40.
[9] Zhang L, Goren MB, Holzer TJ, Andersen BR. Effect of *Mycobacterium tuberculosis*-derived sulfolipid I on human phagocytic cells. Infect Immun 1988;56:2876–83.
[10] Middlebrook G, Dubos RJ, Pierce CJ. Virulence and morphological characteristics of mammalian tubercle bacilli. J Exp Med 1947;86: 175–87.
[11] Yarkoni E, Rapp HJ. Granuloma formation in lungs of mice after intravenous administration of emulsified trehalose-6,6′-dimycolate (cord factor): reaction intensity depends on size distribution of the oil droplets. Infect Immun 1977;18:552–4.
[12] Kunkel SL, Chensue SW, Strieter RM, Lynch JP, Remick DG. Cellular and molecular aspects of granulomatous inflammation. Am J Respir Cell Mol Biol 1989;1:439–47.
[13] Orme IM. The immunopathogenesis of tuberculosis: a new working hypothesis. Trends Microbiol 1998;6:94–7.
[14] Kaneda K, Sumi Y, Kurano F, Kato Y, Yano I. Granuloma formation and hemopoiesis induced by C_{36-48}-mycolic acid-containing glycolipids from *Nocardia rubra*. Infect Immun 1986;54:869–75.
[15] Matsunaga I, Oka S, Fujiwara N, Yano I. Relationship between induction of macrophage chemotactic factors and formation of granulomas caused by mycoloyl glycolipids from *Rhodococcus ruber* (*Nocardia rubra*). J Biochem Tokyo 1996;120:663–70.
[16] Yamagami H, Matsumoto T, Fujiwara N, Arakawa T, Kaneda K, Yano I, et al. Trehalose 6,6′-dimycolate (cord factor) of *Mycobacterium tuberculosis* induces foreign-body- and hypersensitivity-type granulomas in mice. Infect Immun 2001;69:810–5.
[17] Lima VM, Bonato VL, Lima KM, Dos Santos SA, Dos Santos RR, Goncalves ED, et al. Role of trehalose dimycolate in recruitment of cells and modulation of production of cytokines and NO in tuberculosis. Infect Immun 2001;69:5305–12.
[18] Behling CA, Perez RL, Kidd MR, Staton Jr GW, Hunter RL. Induction of pulmonary granulomas, macrophage procoagulant activity, and tumor necrosis factor-alpha by trehalose glycolipids. Ann Clin Lab Sci 1993;23: 256–66.
[19] Bekierkunst A, Levij IS, Yarkoni E. Suppression of urethan-induced lung adenomas in mice treated with trehalose-6,6-dimycolate (cord factor) and living bacillus Calmette Guerin. Science 1971;174:1240–2.
[20] Furukawa M, Ohtsubo Y, Sugimoto N, Katoh Y, Dohi Y. Induction of tumoricidal activated macrophages by a liposome-encapsulated glycolipid, trehalose 2,3,6′-trimycolate from *Gordona aurantiaca*. FEMS Microbiol Immunol 1990;2:83–8.
[21] Orbach-Arbouys S, Tenu JP, Petit JF. Enhancement of in vitro and in vivo antitumor activity by cord factor (6-6′-dimycolate of trehalose) administered suspended in saline. Int Arch Allergy Appl Immunol 1983;71:67–73.
[22] Oswald IP, Dozois CM, Petit JF, Lemaire G. Interleukin-12 synthesis is a required step in trehalose dimycolate-induced activation of mouse peritoneal macrophages. Infect Immun 1997;65:1364–9.
[23] Ryll R, Watanabe K, Fujiwara N, Takimoto H, Hasunuma R, Kumazawa Y, et al. Mycobacterial cord factor, but not sulfolipid, causes depletion of NKT cells and upregulation of CD1d1 on murine macrophages. Microbes Infect 2001;3:611–9.
[24] Ozeki Y, Kaneda K, Fujiwara N, Morimoto M, Oka S, Yano I. In vivo induction of apoptosis in the thymus by administration of mycobacterial cord factor (trehalose 6,6′-dimycolate). Infect Immun 1997;65:1793–9.
[25] Hamasaki N, Isowa K, Kamada K, Terano Y, Matsumoto T, Arakawa T, et al. In vivo administration of mycobacterial cord factor (trehalose 6, 6′-dimycolate) can induce lung and liver granulomas and thymic atrophy in rabbits. Infect Immun 2000;68:3704–9.
[26] Ueda S, Fujiwara N, Naka T, Sakaguchi I, Ozeki Y, Yano I, et al. Structure-activity relationship of mycoloyl glycolipids derived from *Rhodococcus* sp. 4306. Microb Pathog 2001;30:91–9.
[27] Gotoh K, Mitsuyama M, Imaizumi S, Kawamura I, Yano I. Mycolic acid-containing glycolipid as a possible virulence factor of *Rhodococcus equi* for mice. Microbiol Immunol 1991;35:175–85.
[28] Dubnau E, Chan J, Raynaud C, Mohan VP, Laneelle MA, Yu K, et al. Oxygenated mycolic acids are necessary for virulence of *Mycobacterium tuberculosis* in mice. Mol Microbiol 2000;36:630–7.
[29] Valway SE, Sanchez MP, Shinnick TF, Orme I, Agerton T, Hoy D, et al. An outbreak involving extensive transmission of a virulent strain of *Mycobacterium tuberculosis*. N Engl J Med 1998;338:633–9.
[30] Manca C, Tsenova L, Barry III CE, Bergtold A, Freeman S, Haslett PA, et al. *Mycobacterium tuberculosis* CDC1551 induces a more vigorous host response in vivo and in vitro, but is not more virulent than other clinical isolates. J Immunol 1999;162:6740–6.
[31] Manca C, Tsenova L, Bergtold A, Freeman S, Tovey M, Musser JM, et al. Virulence of a *Mycobacterium tuberculosis* clinical isolate in mice is determined by failure to induce Th1 type immunity and is associated with induction of IFN-alpha/beta. Proc Natl Acad Sci USA 2001;98:5752–7.
[32] Manca C, Reed MB, Freeman S, Mathema B, Kreiswirth B, Barry III CE, et al. Differential monocyte activation underlies strain-specific *Mycobacterium tuberculosis* pathogenesis. Infect Immun 2004;72:5511–4.
[33] Sumi Y, Kurano S, Kato Y, Sawai H, Tomiyasu I, Kaneda K, et al. Strain differences in granuloma formation in mice in response to mycolic acid-containing glycolipids of some species of *Nocardia* and *Rhodococcus*. Nippon Saikingaku Zasshi 1986;41:797–804.
[34] Adams JL, Czuprynski CJ. Mycobacterial cell wall components induce the production of TNF-alpha, IL-1, and IL-6 by bovine monocytes and the murine macrophage cell line RAW 264.7. Microb Pathog 1994;16: 401–11.
[35] Adams JL, Czuprynski CJ. Ex vivo induction of TNF-alpha and IL-6 mRNA in bovine whole blood by *Mycobacterium paratuberculosis* and mycobacterial cell wall components. Microb Pathog 1995;19:19–29.
[36] Horgen L, Barrow EL, Barrow WW, Rastogi N. Exposure of human peripheral blood mononuclear cells to total lipids and serovar-specific glycopeptidolipids from *Mycobacterium avium* serovars 4 and 8 results in inhibition of TH1-type responses. Microb Pathog 2000;29:9–16.
[37] Goren MB, Brokl O, Schaefer WB. Lipids of putative relevance to virulence in *Mycobacterium tuberculosis*: correlation of virulence with elaboration of sulfatides and strongly acidic lipids. Infect Immun 1974;9: 142–9.
[38] Goren MB, Grange JM, Aber VR, Allen BW, Mitchison DA. Role of lipid content and hydrogen peroxide susceptibility in determining the guinea-pig virulence of *Mycobacterium tuberculosis*. Br J Exp Pathol 1982;63: 693–700.
[39] Grange JM, Aber VR, Allen BW, Mitchison DA, Goren MB. The correlation of bacteriophage types of *Mycobacterium tuberculosis* with guinea-pig virulence and in vitro-indicators of virulence. J Gen Microbiol 1978;108:1–7.
[40] Watanabe K, Hasunuma R, Horikoshi T, Yamana H, Maruyama H, Fujiwara N, et al. Induction of hypersensitivity to endotoxin lethality in mice by treatment with trehalose 6,6′-dimycolate but not with 2,3,6,6′-tetraacyl trehalose 2′-sulfate. J Endotoxin Res 1999;5:23–30.
[41] Bean AG, Roach DR, Briscoe H, France MP, Korner H, Sedgwick JD, et al. Structural deficiencies in granuloma formation in TNF gene-targeted mice underlie the heightened susceptibility to aerosol *Mycobacterium tuberculosis* infection, which is not compensated for by lymphotoxin. J Immunol 1999;162:3504–11.

[42] Ehlers S. Role of tumour necrosis factor (TNF) in host defence against tuberculosis: implications for immunotherapies targeting TNF. Ann Rheum Dis 2003;62:ii37–42.
[43] Flynn JL, Goldstein MM, Chan J, Triebold KJ, Pfeffer K, Lowenstein CJ, et al. Tumor necrosis factor-alpha is required in the protective immune response against *Mycobacterium tuberculosis* in mice. Immunity 1995;2: 561–72.
[44] Kaneko H, Yamada H, Mizuno S, Udagawa T, Kazumi Y, Sekikawa K, et al. Role of tumor necrosis factor-alpha in *Mycobacterium*-induced granuloma formation in tumor necrosis factor-alpha-deficient mice. Lab Invest 1999;79:379–86.
[45] Kindler V, Sappino AP, Grau GE, Piguet PF, Vassalli P. The inducing role of tumor necrosis factor in the development of bactericidal granulomas during BCG infection. Cell 1989;56:731–40.
[46] Roach DR, Bean AG, Demangel C, France MP, Briscoe H, Britton WJ. TNF regulates chemokine induction essential for cell recruitment, granuloma formation, and clearance of mycobacterial infection. J Immunol 2002;168:4620–7.
[47] Flynn JL, Scanga CA, Tanaka KE, Chan J. Effects of aminoguanidine on latent murine tuberculosis. J Immunol 1998;160:1796–803.
[48] Adams LB, Mason CM, Kolls JK, Scollard D, Krahenbuhl JL, Nelson S. Exacerbation of acute and chronic murine tuberculosis by administration of a tumor necrosis factor receptor-expressing adenovirus. J Infect Dis 1995;171:400–5.
[49] Mohan VP, Scanga CA, Yu K, Scott HM, Tanaka KE, Tsang E, et al. Effects of tumor necrosis factor alpha on host immune response in chronic persistent tuberculosis: possible role for limiting pathology. Infect Immun 2001;69:1847–55.
[50] Middlebrook G, Coleman CM, Schaefer WB. Sulfolipid from virulent tubercle bacilli. Proc Natl Acad Sci USA 1959;45:1801–4.
[51] Rousseau C, Turner OC, Rush E, Bordat Y, Sirakova TD, Kolattukudy PE, et al. Sulfolipid deficiency does not affect the virulence of *Mycobacterium tuberculosis* H37Rv in mice and guinea pigs. Infect Immun 2003;71:4684–90.
[52] Sirakova TD, Thirumala AK, Dubey VS, Sprecher H, Kolattukudy PE. The *Mycobacterium tuberculosis pks2* gene encodes the synthase for the hepta- and octamethyl-branched fatty acids required for sulfolipid synthesis. J Biol Chem 2001;276:16833–9.
[53] Yano I, Tomiyasu I, Kitabatake S, Kaneda K. Granuloma forming activity of mycolic acid-containing glycolipids in *Nocardia* and related taxa. Acta Leprol 1984;2:341–9.
[54] Carswell EA, Old LJ, Kassel RL, Green S, Fiore N, Williamson B. An endotoxin-induced serum factor that causes necrosis of tumors. Proc Natl Acad Sci USA 1975;72:3666–70.
[55] Aggarwal BB, Kohr WJ, Hass PE, Moffat B, Spencer SA, Henzel WJ, et al. Human tumor necrosis factor. Production, purification, and characterization. J Biol Chem 1985;260:2345–54.

Molecular Microbiology (2007) 63(4), 1096–1106
doi:10.1111/j.1365-2958.2006.05585.x
First published online 18 January 2007

Loss of a conserved 7-methylguanosine modification in 16S rRNA confers low-level streptomycin resistance in bacteria

Susumu Okamoto,[1] Aki Tamaru,[2] Chie Nakajima,[3] Kenji Nishimura,[1,4] Yukinori Tanaka,[1,4] Shinji Tokuyama,[4] Yasuhiko Suzuki[3] and Kozo Ochi[1*]

[1]*Microbial Function Laboratory, National Food Research Institute, 2-1-12 Kannondai, Tsukuba, Ibaraki 305-8642, Japan.*
[2]*Bacteriology Division, Osaka Prefectural Institute of Public Health, 1-3-69 Nakamichi, Higashinari-ku, Osaka 537-0025, Japan.*
[3]*Department of Global Epidemiology, Research Center for Zoonosis Control, Hokkaido University, Kita 18, Nishi 9, Kita-ku, Sapporo 060-0818, Japan.*
[4]*Department of Applied Biological Chemistry, Faculty of Agriculture, Shizuoka University, 836 Ohya, Shizuoka 422-8529, Japan.*

Summary

Streptomycin has been an important drug for the treatment of tuberculosis since its discovery in 1944. But numerous strains of *Mycobacterium tuberculosis*, the bacterial pathogen that causes tuberculosis, are now streptomycin resistant. Although such resistance is often mediated by mutations within *rrs*, a 16S rRNA gene or *rpsL*, which encodes the ribosomal protein S12, these mutations are found in a limited proportion of clinically isolated streptomycin-resistant *M. tuberculosis* strains. Here we have succeeded in identifying a mutation that confers low-level streptomycin resistance to bacteria, including *M. tuberculosis*. We found that mutations within the gene *gidB* confer low-level streptomycin resistance and are an important cause of resistance found in 33% of resistant *M. tuberculosis* isolates. We further clarified that the *gidB* gene encodes a conserved 7-methylguanosine (m^7G) methyltransferase specific for the 16S rRNA, apparently at position G527 located in the so-called 530 loop. Thus, we have identified *gidB* as a new streptomycin-resistance locus and uncovered a resistance mechanism that is mediated by loss of a conserved m^7G modification in 16S rRNA. The clinical significance of *M. tuberculosis gidB* mutation also is noteworthy, as *gidB* mutations emerge spontaneously at a high frequency of 10^{-6} and, once emerged, result in vigorous emergence of high-level streptomycin-resistant mutants at a frequency more than 2000 times greater than that seen in wild-type strains. Further studies on the precise function of GidB may provide a basis for developing strategies to suppress pathogenic bacteria, including *M. tuberculosis*.

Accepted 21 December, 2006. *For correspondence. E-mail kochi@affrc.go.jp; Tel. (+81) 29 838 8125; Fax (+81) 29 838 7996.

Introduction

Selman Waksman discovered streptomycin to be a particularly potent drug against *Mycobacterium tuberculosis* in 1944, while at Rutgers University (Schatz and Waksman, 1944). The first mutants resistant to streptomycin were reported as early as 1946 (Klein and Kimmelman, 1946). The mutants could be classified into two distinct types, depending upon whether they exhibit high- or low-level streptomycin resistance.

Because of its clinical importance, molecular mechanisms of resistance to streptomycin have been extensively studied, especially in *M. tuberculosis* (Finken *et al.*, 1993; Nair *et al.*, 1993; Honoré and Cole, 1994; Honoré *et al.*, 1995; Carter *et al.*, 2000; Ogle and Ramakrishnan, 2005). However, the genetic basis of resistance is still not fully understood. High-level streptomycin resistance is often linked to mutations within *rrs*, a 16S rRNA gene, or *rpsL*, which encodes the ribosomal protein S12 (Finken *et al.*, 1993; Nair *et al.*, 1993; Honoré and Cole, 1994; Honoré *et al.*, 1995). Most mutations within S12 that confer resistance to, or dependence on, streptomycin are known to lead to a hyperaccurate phenotype (Carter *et al.*, 2000), which compensates for the effect of the drug, without affecting the interaction between the drug and the ribosome. A number of mutations within 16S rRNA, including those within the so-called 530 loop, also lead to both streptomycin resistance and hyperaccuracy (Montandon *et al.*, 1986; Powers and Noller, 1991; Pinard *et al.*, 1993). Such changes, however, have been identified in a limited

Table 1. Frequency of *gidB* mutants in several bacteria.[a]

Strain	Sm concentration (μg ml^{-1})		Frequency of Sm^r mutants	Frequency of *gidB* mutants
	MIC	Mutant selection		
Escherichia coli	2	5	2.0×10^{-5}	4/39
Staphylococcus aureus	3	10	1.2×10^{-5}	4/16
Mycobacterium smegmatis	0.3	1	2.3×10^{-4}	17/18
Mycobacterium tuberculosis	1	2	2.8×10^{-6}	10/10

a. For mutant isolation, the media used were LB (for *E. coli* and *S. aureus*), R (for *M. smegmatis*) and Middlebrook 7H11 [for *M. tuberculosis* (No. 05–048)].
Sm, streptomycin; Sm^r, streptomycin resistant. Frequencies of *gidB* mutants are expressed as the (number of *gidB* mutants)/(number of Sm^r mutants sequenced).

proportion (i.e. just over one-half) of clinically isolated streptomycin-resistant *M. tuberculosis* strains studied to date (Meier *et al.*, 1996; Sreevatsan *et al.*, 1996; Gillespie, 2002; Ramaswamy *et al.*, 2004). Consequently, the mechanism underlying low-level resistance to streptomycin has remained obscure for 60 years (Demerec, 1948).

We describe here our identification of an unknown mutation within *gidB* that confers low-level streptomycin resistance. Subsequent analysis of this mutation demonstrated both its clinical importance and its potential to further our understanding of the mechanism underlying the development of high-level streptomycin resistance in *M. tuberculosis*, thus providing basis for developing strategies to suppress this serious pathogenic bacterium.

Results

Low-level streptomycin resistance caused by gidB *mutations*

Our laboratory has focused on unravelling unknown ribosomal functions, thus aiming to develop 'ribosome engineering' (Ochi *et al.*, 2004) as a rational approach to taking full advantage of bacterial capabilities. The members of the genus *Streptomyces* are distinguished in the ability to exert a wide variety of secondary metabolisms as represented by antibiotic production. The ability of *Streptomyces coelicolor* A3(2) to produce antibiotics is dramatically enhanced by introducing mutations that confer high- or low-level resistance to streptomycin (Shima *et al.*, 1996; Hosoya *et al.*, 1998; Okamoto *et al.*, 2003; Ochi *et al.*, 2004; Hosaka *et al.*, 2006). To study the mechanism by which mutations causing low-level streptomycin resistance induce gene activation, we first conducted genetic analysis (i.e. mapping of the mutations on the chromosome) (Ochi and Hosoya, 1998). Because of the apparent failure of conventional cloning strategies to identify the mutations, we next used comparative genome sequencing (CGS) (Albert *et al.*, 2005), a microarray hybridization-based method developed to search for single nucleotide polymorphisms (SNPs) and insertion–deletion sites within the genome. The mutant (*relA str-1*) strain, showing low-level streptomycin resistance due to *str-1* mutation, served for analysis. Because the *str-1* mutation had previously been mapped to the 7 o'clock position on the *S. coelicolor* chromosome (Ochi and Hosoya, 1998), CGS was conducted for 1.2 Mbp around the 7 o'clock region. This analysis enabled us to identify a putative SNP within the gene *gidB*, which was confirmed to be a deletion mutation (deletion of 488 A) by DNA sequencing (details will be reported elsewhere).

The *gidAB* operon was originally described in *Escherichia coli* in relation to glucose-mediated inhibition of cell division (von Meyenburg and Hansen, 1980). Subsequent analysis revealed that inactivation of *gidA* (but not *gidB*) is responsible for impaired cell division in the presence of glucose (von Meyenburg and Hansen, 1980), and more recent data support the involvement of *gidA* in tRNA modification (Brégeon *et al.*, 2001; Yim *et al.*, 2006). On the other hand, function of *gidB* has remained obscure to date. The *gidB* gene is highly conserved in both Gram-positive and Gram-negative bacteria (Fig. S1) and is found in all bacterial genomes sequenced to date, including that of *Mycoplasma genitalium*, the smallest genome of a known self-sustaining living organism. We therefore suspected that *gidB* mutations may cause low-level streptomycin resistance in virtually all bacteria. To address this possibility, we examined the emergence of streptomycin-resistant mutants in several bacteria on plates containing a low concentration of streptomycin [two to three times the minimum inhibitory concentration (MIC)] (Table 1). We found that streptomycin-resistant mutants emerged at a high frequency, in the order of 10^{-4} or 10^{-5}, in *E. coli*, *Staphylococcus aureus* and *Mycobacterium smegmatis*, and in the order of 10^{-6} in *M. tuberculosis* (Table 1). In addition, there was a high incidence of *gidB* mutations in these strains. For example, in *M. smegmatis* and *M. tuberculosis*, almost all mutants carried *gidB* mutations (17/18 and 10/10 respectively), including a variety of point, deletion and insertion mutations (see Table S1), suggesting loss of function of *gidB* may result in a streptomycin-resistant phenotype.

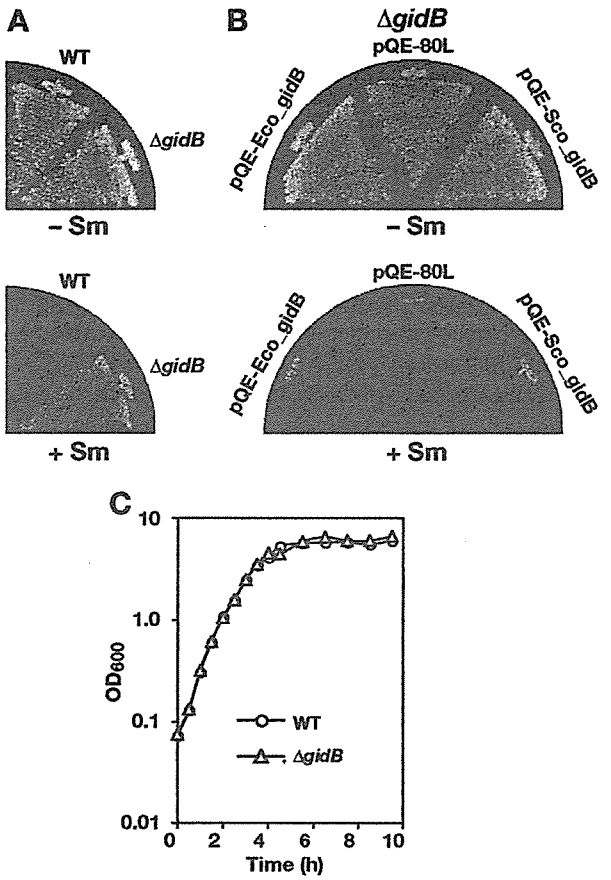

Fig. 1. Mutation of *gidB* confers streptomycin resistance.
A. Streptomycin-resistant phenotype of the *E. coli* Δ*gidB* mutant. Wild-type and Δ*gidB* strains were streaked onto LB (–Sm) or LB containing 10 μg ml^{-1} streptomycin (+Sm).
B. Complementation of the Δ*gidB* mutant. *E. coli* or *S. coelicolor* GidB was expressed as a His-tagged protein using pQE-80L. Strains were grown on LB agar containing ampicillin, either in the absence (–Sm) or presence (+Sm) of streptomycin (8 μg ml^{-1}).
C. Growth of Δ*gidB* mutant, as compared with the wild-type strain. Cultures were grown in LB medium at 37°C.

To verify a causal relationship between *gidB* mutation and streptomycin resistance, we compared wild-type *E. coli* BW25113 and its isogenic *gidB* deletion (Δ*gidB*) mutant. We found that the streptomycin MIC for the wild-type strain was 2 μg ml^{-1}, whereas the Δ*gidB* mutant remained viable at concentrations up to 15 μg ml^{-1}, suggesting that the *gidB* mutation is indeed responsible for streptomycin resistance (Fig. 1A). This was confirmed by our finding that introduction of a plasmid containing the wild-type *gidB* into Δ*gidB* cells completely eliminated the resistance to streptomycin (Fig. 1B). Likewise, *gidB* from *S. coelicolor* also effectively complemented the *E. coli* *gidB* mutation. Apparently, the proteins encoded by both *gidB* genes were functionally equivalent and involved in the same biochemical pathway(s). The *gidB* mutant also showed no changes in susceptibility to ribosome-targeting antibiotics, such as erythromycin, tetracycline, chloramphenicol and spectinomycin (data not shown).

Certain drug-resistant bacteria grow more slowly than susceptible bacteria because the mutations that confer resistance also reduce the overall fitness of the organism (Andersson and Levin, 1999), a phenomenon known as 'cost of resistance'. We found, however, that the *E. coli* Δ*gidB* mutant grew as well as the parent strain in both nutritional media (Fig. 1C) and chemically defined media (data not shown).

GidB functions as an rRNA methyltransferase

The GidB protein has a putative *S*-adenosyl-L-methionine (SAM)-binding motif within its primary structure (Fig. S1) (Kagan and Clarke, 1994), and the crystal structure of *E. coli* GidB showed that it contains a SAM-dependent methyltransferase fold within its ternary structure (Romanowski *et al.*, 2002). As streptomycin resistance often results from mutations that affect ribosome-associated components (Cundliffe, 1990), we hypothesized that *gidB* mutants also have an altered ribosome – i.e. a deficiency in the methylation of some ribosomal component(s), which generates streptomycin resistance. We tested this hypothesis by measuring the protein synthetic activity of ribosomes *in vitro* (Fig. 2). Green fluorescent protein (GFP) was synthesized using ribosomes and the S-150 fractions from the wild-type and the Δ*gidB*

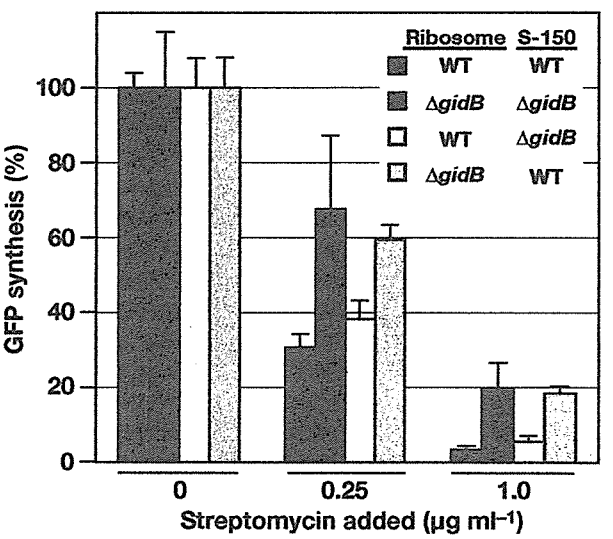

Fig. 2. Effect of streptomycin on *in vitro* protein synthesis. Ribosome and S-150 fractions were prepared from wild-type (streptomycin susceptible) and Δ*gidB* (streptomycin resistant) *E. coli* strains. Reactions were performed using the four possible combinations of ribosome and S-150 fractions. Streptomycin was added to the reaction mixture at the indicated concentrations. The production of GFP was measured, and the results are presented as the mean per cent translational activity ± SD, with 100% defined as activity in the absence of the drug.

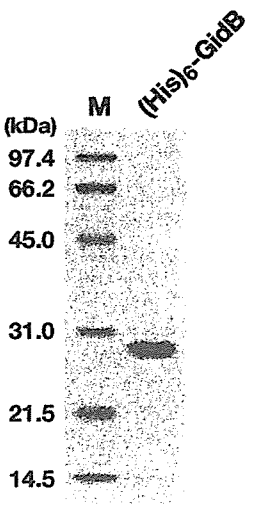

Fig. 3. SDS-PAGE of the purified $(His)_6$-GidB protein. Two micrograms of the protein was subjected to 12% SDS-PAGE. M represents marker proteins.

strains in the presence or absence of streptomycin. By cross-mixing the components, we determined that the ribosome itself, not the S-150 fraction, is responsible for streptomycin resistance.

We next determined the ribosomal target for the presumptive methyltransferase GidB. We therefore prepared an N-terminal His-tagged GidB and purified it using immobilized metal ion chromatography (Fig. 3). To determine whether the recombinant GidB was able to catalyse ribosomal modification, 70S ribosomes from the wild-type or Δ*gidB* strain were incubated in the presence of purified GidB and [*methyl*-^{3}H]SAM, and incorporation of methyl groups was analysed by trichloroacetic acid precipitation or fluorography of polyacrylamide gels. When ribosomes from Δ*gidB* cells were used as a substrate, a significant amount of methyl groups were incorporated (Fig. 4A). By contrast, no incorporation was detected when ribosomes from the wild-type cells were used, presumably reflecting the already saturated methylation status of those ribosomes. Moreover, using rRNA extraction and subsequent non-denaturing polyacrylamide gel electrophoresis, we determined that the methylated ribosomal component was the 16S rRNA (Fig. 4B). This was confirmed by per-

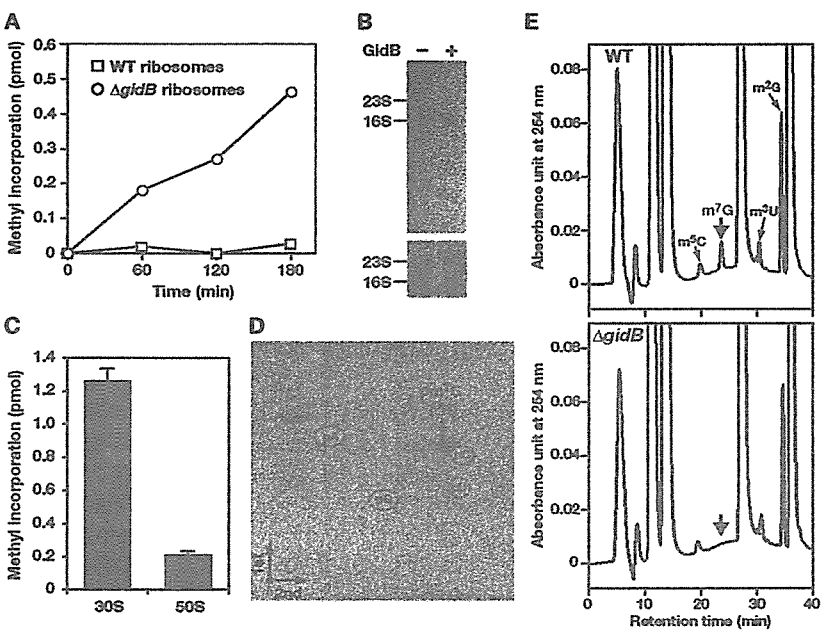

Fig. 4. GidB is a m^7G methyltransferase specific for 16S rRNA.
A. Methyl acceptor activity of wild-type and mutant ribosomes. 70S ribosomes (1 μM) prepared from either the wild-type (open squares) or Δ*gidB* (open circles) *E. coli* strain were subjected to methylation using [^{3}H]-SAM (3 μM) and the purified $(His)_6$-GidB protein (500 nM).
B. Methylation of 16S rRNA by GidB. Δ*gidB* 70S ribosomes were methylated using [^{3}H]-SAM and $(His)_6$-GidB, after which rRNAs were extracted and analysed on 3.5% non-denaturing polyacrylamide gels. Fluorography (upper panel) and RNA staining (lower panel) are shown.
C. Methylation of the 30S ribosomal subunit by GidB. The 30S and 50S ribosomal subunits from the Δ*gidB* strain were used as the substrates. Values are means ± SD.
D. Determination of the methylated nucleotide by 2D-TLC. Radiolabelled nucleotides were detected using fluorography. Dotted circles show the migration of the four canonical nucleotides used as UV markers.
E. *E. coli* Δ*gidB* strain lacks m^7G modification in 16S rRNA. 16S rRNAs from the wild-type (upper panel) and Δ*gidB* (lower panel) strains were isolated, digested completely to nucleosides and analysed by HPLC. The peaks for m^7G, m^5C, m^2G and m^3U are indicated by arrows.

